PHYSICAL REVIEW B VOLUME 27, NUMBER 8 15 APRIL 1983

Theory of photodesorption of molecules by resonant laser-molecular vibrational coupling

Z. W. Gortel and H. J. Kreuzer
Department of Physics, Dalhousie University, Halifax, Nova Scotia B3H 3J5, Canada

P. Piercy and R. Teshima
Department of Physics, University of Alberta, Edmonton, Alberta T6G 2J1, Canada
(Received 28 October 1982)

Photodesorption due to a laser resonantly coupled into an internal vibrational mode of an adsorbed molecule is considered. Based on a master equation with transition probabilities calculated quantum statistically for laser-induced vibrational transitions, phonon-mediated bound-state—bound-state and bound-state—continuum transitions, and tunneling transitions from bound states degenerate with the continuum, we calculate desorption rates as a function of temperature and laser intensity. They are highly nonlinear in both, and become saturated for high intensities. The theory is applied to the CH_3F-NaCl and CO-NaCl systems.

I. INTRODUCTION

A laser beam impinging onto an adsorbate-covered surface of a solid can deposit all or part of its energy either (a) into the solid directly, (b) into the surface bond with which an adsorbed molecule is bound to the surface, or (c) into some internal vibrational or rotational mode of the adsorbed molecule. Process (a) will heat up the solid leading to thermal desorption: We speak of direct laser-induced thermal desorption. Its feasibility was demonstrated by Levine *et al.*[1,2] and by Ertl and Neumann[3–5] after many inconclusive attempts by others. In a recent study of this kind on the Co-Fe system in which time of flight spectra of the desorbed molecules are analyzed in great detail, Wedier and Ruhmann,[6] reach surface temperatures of about 1000 °C within the duration of nanoseconds (ns) of a pulsed Nd laser at intensities up to 30 mW/cm^2.

Whereas direct laser-induced thermal desorption is possible at all laser frequencies at which appreciable absorption of light occurs in the solid, processes (b) and (c) are resonant in character. To understand (b) we recall that, at least in physisorption, we can envisage the adsorbed molecule to sit in the attractive trough of a surface potential V_s which represents the net interaction between the molecule and the solid. Its long-range attractive part is essentially the interaction energy between the mutually-induced fluctuating dipole moments on the adsorbed gas particle and in the solid. This surface potential V_s will in general develop several bound states $E_0,\ldots,E_n$ into which gas molecules can become trapped to form the adsorbate. For most adsorbates there is also a net charge transfer between the solid and the adsorbed molecule, very pronounced, e.g., in the adsorption of alkali or halogen atoms on metals. The electromagnetic field of the laser can couple into the resulting dipole, promoting an adsorbed molecule from a surface bound state E_i to E_j if the laser frequency is close to resonance $\hbar\Omega_l = E_j - E_i$. Let us therefore tune a laser such that one photon lifts a molecule from E_0 to E_j, say. At high-enough laser intensity further absorption of photons can occur provided that a surface bound state is available at energy $E_{j'} = E_j + \hbar\Omega_l$. Because the surface potential is very anharmonic, particularly at the top, this is very unlikely, except if these states E_j are broadened considerably as Jedrzejek *et al.*[7] postulate it for CO on Cu, a system for which further adsorption of a third photon lifts the molecule into a continuum state, i.e., desorbs it. We call this process (b) photodesorption by laser—surface-bond coupling.[8] Higher-order processes like the simultaneous absorption of a photon and emission or absorption of a phonon can also lead to overall energy conservation but that seems quite unlikely.

Next we consider process (c) in which we assume that a laser is resonantly coupled into an internal vibrational mode of the adsorbed molecule, which for the lowest few excited states we assume to be adequately described by a harmonic oscillator of frequency Ω. Because $\hbar\Omega$ is typically much larger than the spacing between the energies $(E_{i+1} - E_i)$ of bound states in the surface potential, we can, in a first approximation, assume that the internal degrees of freedom of the molecule are decoupled from its interaction with the surface. At low temperatures an adsorbed molecule will then be in the ground state of energy

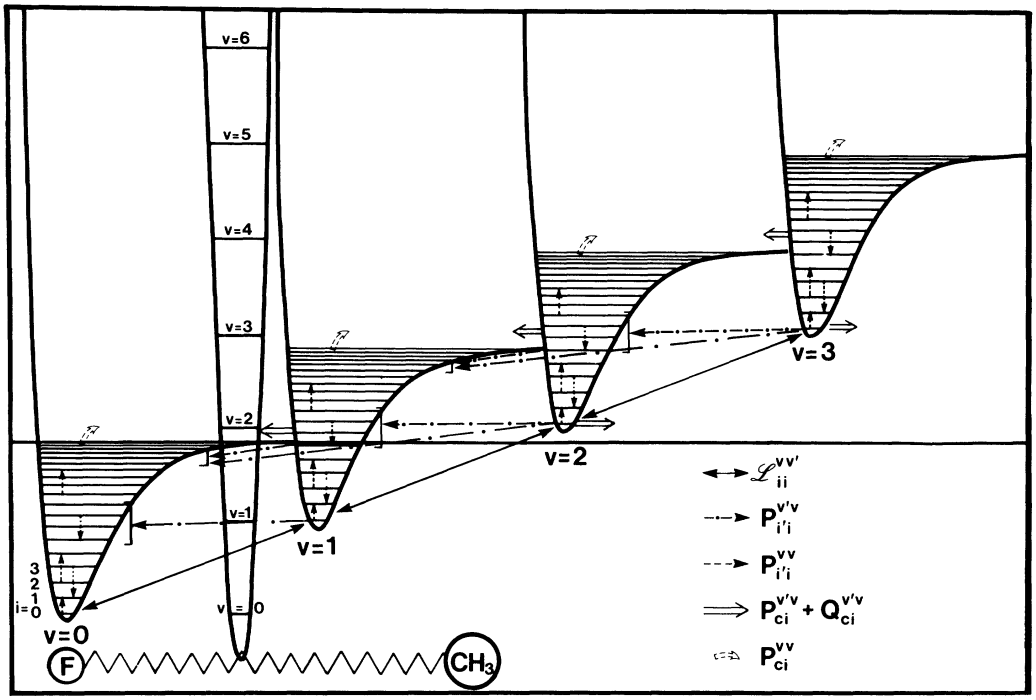

FIG. 1. Schematic energy diagram of a molecule adsorbed on a surface with some of the processes included in the theory indicated by arrows with the following transition probabilities: $P_{i'i}^{v'v}$ indicates the phonon-mediated bound state–bound state: $(i,v)\rightarrow(i',v')$; $P_{ci}^{v'v}$ is the phonon-mediated bound state–continuum; $Q_{ci}^{v'v}$ indicates elastic tunneling into continuum; $\mathscr{L}_{ii}^{v'v}$ indicates laser coupling.

$$E_i^v = E_0^0 = E_0 + \tfrac{1}{2}\hbar\Omega$$

where i labels the bound states in the surface potential and v counts the quanta excited in the internal vibrational mode of the molecule. Upon absorption of a laser photon the molecule will be in a state E_0^1 from which it can either absorb more photons to go up to higher v or emit a phonon of energy $\hbar\omega$ such that $E_i^0 = E_0^1 + \hbar\omega$. It is then in an excited state of the surface potential from which it can cascade down to $i=0$, emitting more phonons and thus heating up the solid. This process one might call resonant heating. If effective enough it can lead to thermal desorption (see Fig. 1).

If a molecule can be excited into a higher internal vibrational state such that its total energy

$$E_0^v = p^2/2m + (v' + \tfrac{1}{2})\,\hbar\Omega$$

is degenerate with some continuum state of momentum p (with v' possibly zero) then elastic tunneling into the latter state will desorb the molecule. This process has been examined by Lucas and Ewing.[9] Tunneling can also be inelastic, i.e., aided by the emission and adsorption of phonons, a process investigated by Kreuzer and Lowy.[10] We will refer to both elastic and inelastic tunneling processes as photodesorption by resonant laser-molecule vibrational coupling. Its feasibility has been demonstrated by Heidberg *et al.*[11–13] for the system CH_3F on NaCl and by Chuang[14,15] for pyridine on KCl and silver.

In the next two sections we will set up the Hamiltonian for a molecule adsorbed on the surface of a solid interacting with its phonon field and with the photon field of an incident laser beam. For the latter it is obviously necessary to know the local electric and magnetic fields within a few angstroms of the surface of the solid. For a dielectric a good case can be made to calculate the local fields according to the classical Fresnel formulas, which seem to be applicable even at the surface of a metal that is covered by a monolayer adsorbate treated as a thin dielectric sheet.[16] The theory predicts in this case a high absorption coefficient for light close to grazing incidence, i.e., incident under an angle of 80°–90° to the surface normal, a fact that is used in infrared reflection-absorption spectroscopy of adsorbed atoms and molecules.[17] On the other hand, the local laser field at a metal surface with much less than a monolayer of adsorbed molecules seems to be amplified by many orders of magnitude as inferred from extraordinarily large surface Raman scattering, particularly on silver surfaces.[18] A number of greatly varying explanations are currently discussed in the

literature.[19] We will restrict our numerical results in this paper to dielectrics for which the local fields are evaluated in the Appendix.

In Sec. IV we set up the master equation controlling the time evolution of the occupation functions of the states E_i^v of an adsorbed molecule with transition probabilities calculated according to Fermi's golden rule for the laser-induced dipole transitions in the molecule, for the phonon-induced cascades in the surface potential, for the resonant heating mechanism, and for the elastic and inelastic tunneling processes into continuum states leading eventually to desorption. These calculations can be done analytically if one chooses for the surface potential a one-dimensional Morse potential.

In Sec. IV we present the numerical calculations of photodesorption rates as a function of solid temperature and laser fluence, the latter being the surface density of the energy deposited by the laser pulse, i.e., the time integral of its intensity. The two systems studied are CH_3F on NaCl and CO on NaCl; for the former experimental results have been published by Heidberg *et al.*[11–13] Section VI presents some final comments and an outlook to future work.

II. STATIC GAS-SOLID SYSTEM

In the photodesorption of molecules by resonant laser-molecular vibrational coupling only one internal degree of freedom of the molecule plays an active part, namely that vibration into which the laser is coupled resonantly. We can therefore treat the polyatomic molecule as consisting of two inert parts A and B vibrating against each other with some frequency Ω. In a diatomic molecule like CO, A and B are simply atoms; for CH_3F, one identifies A with F and B with the CH_3 radical with $\Omega=\nu_3$.

We write the Hamiltonian of the gas-solid system as

$$H=H_g+H_s+H_l+H_{\rm dyn} , \tag{1}$$

where H_g is the Hamiltonian of the molecular gas in front of a static surface, H_s contains the phonon degrees of freedom of the solid, H_l describes the free radiation field of the laser, and $H_{\rm dyn}$ couples these sets of degrees of freedom together. In this section we deal with H_g only and write

$$H_g=-\frac{\hbar^2}{2m_A}\frac{\partial^2}{\partial\vec{x}_A^{\,2}}-\frac{\hbar^2}{2m_B}\frac{\partial^2}{\partial\vec{x}_B^{\,2}} +U(|\vec{x}_A-\vec{x}_B|) +V_s^{(A)}(\vec{x}_A)+V_s^{(B)}(\vec{x}_B) , \tag{2}$$

where U is the harmonic-oscillator potential for the active vibrational degree of freedom of the molecule. $V_s^{(A)}$ is the effective surface potential felt by the A part of the molecule and $V_s^{(B)}$ is the same for the B part. We introduce center-of-mass and relative coordinates,

$$\begin{aligned} m\vec{x}&=m_A\vec{x}_A+m_B\vec{x}_B ,\\ \vec{\xi}&=\vec{x}_B-\vec{x}_A ,\\ m&=m_A+m_B , \end{aligned} \tag{3}$$

and also the reduced mass μ, with

$$\mu^{-1}=m_A^{-1}+m_B^{-1} , \tag{4}$$

to get

$$H_g=-\frac{\hbar^2}{2m}\frac{\partial^2}{\partial\vec{x}^{\,2}}-\frac{\hbar^2}{2\mu}\frac{\partial^2}{\partial\vec{\xi}^{\,2}} +U(\xi)+V_s^{(A)}\left[\vec{x}-\frac{\mu}{m_A}\vec{\xi}\right] +V_s^{(B)}\left[\vec{x}+\frac{\mu}{m_B}\vec{\xi}\right] . \tag{5}$$

The Hamiltonian has eigenfunctions and eigenvalues given by the Schrödinger equation,

$$H_g\phi_i^v(\vec{x},\vec{\xi})=E_i^v\phi_i^v(\vec{x},\vec{\xi}) . \tag{6}$$

Introducing field operators $\psi(\vec{x},\vec{\xi},t)$ and expanding them in the complete set of eigenfunctions,

$$\psi(\vec{x},\vec{\xi},t)=\sum_{i,v}\phi_i^v(\vec{x},\vec{\xi})a_i^v(t) , \tag{7}$$

we may express the Hamiltonian operator in second quantized form as

$$\hat{H}_g=\int\psi^\dagger(\vec{x},\vec{\xi},t)H_g\psi(\vec{x},\vec{\xi},t)d\vec{x}\,d\vec{\xi} =\sum_{i,v}E_i^v a_i^{v\dagger}a_i^v . \tag{8}$$

The operators $a_i^{v\dagger}$ and a_i^v create and destroy normal modes of excitations in the system described by H_g, with quantum labels i and v.

We next observe that the energy levels of U are typically much more widely spaced than those in the surface potentials $V_s^{(A)}$ and $V_s^{(B)}$ so that, in lowest approximation, we can replace $\vec{\xi}$ in the latter by the equilibrium separation $\vec{\xi}_0$ of the A and B parts in the molecule. Defining

$$H_m(\vec{x})=-\frac{\hbar^2}{2m}\frac{\partial^2}{\partial\vec{x}^{\,2}}+V_s^{(A)}\left[\vec{x}-\frac{\mu}{m_A}\vec{\xi}_o\right] +V_s^{(B)}\left[\vec{x}+\frac{\mu}{m_B}\vec{\xi}_0\right] , \tag{9}$$

$$H_v(\vec{\xi})=-\frac{\hbar^2}{2\mu}\frac{\partial^2}{\partial\vec{\xi}^2}+U(\xi)\ , \tag{10}$$

$$H_{\rm res}(\vec{x},\vec{\xi})=V_s^{(A)}\left[\vec{x}-\frac{\mu}{m_A}\vec{\xi}\right]-V_s^{(A)}\left[\vec{x}-\frac{\mu}{m_A}\vec{\xi}_0\right]+V_s^{(B)}\left[\vec{x}+\frac{\mu}{m_B}\vec{\xi}\right]-V_s^{(B)}\left[\vec{x}+\frac{\mu}{m_B}\vec{\xi}_0\right]\ , \tag{11}$$

we have

$$H_g(\vec{x},\vec{\xi})=H_m(\vec{x})+H_v(\vec{\xi})+H_{\rm res}(\vec{x},\vec{\xi})\ . \tag{12}$$

If we neglect $H_{\rm res}$ for a moment, the quantum numbers i refer to the center of mass Hamiltonian H_m of the molecule as a whole in the surface potential, enumerating the bound states and the continuum states. Molecules trapped in the bound states form the adsorbate; those in continuum states make up the gas phase. The quantum number v labels the linear harmonic-oscillator states of the internal molecular vibration, so that in this approximation

$$E_i^v\approx E_i+(v+\tfrac{1}{2})\hbar\Omega\ , \tag{13}$$

$$\phi_i^v(\vec{x},\vec{\xi})\approx\phi_i(\vec{x})u_v(\vec{\xi})\ , \tag{14}$$

where

$$H_m\phi_i=E_i\phi_i\ , \tag{15}$$

$$H_v u_v=(v+\tfrac{1}{2})\hbar\Omega u_v\ . \tag{16}$$

Equation (7) then reads

$$\psi(\vec{x},\vec{\xi},t)=\sum_{i,v}\phi_i(\vec{x})u_v(\vec{\xi})\alpha_i^v(t)\ , \tag{17}$$

so that (12) becomes in second quantization

$$\hat{H}_g=\hat{H}_g^{(0)}+\hat{H}_{\rm res}\ , \tag{18}$$

where

$$\hat{H}_g^{(0)}=\sum_{i,v}E_i^v\alpha_i^{v\dagger}\alpha_i^v\ , \tag{19}$$

$$\hat{H}_{\rm res}=\sum_{\substack{ii'\\vv'}}\int d\vec{x}\,d\vec{\xi}\,\phi_i^*(\vec{x})u_v^*(\vec{\xi})H_{\rm res}(\vec{x},\vec{\xi})\times\phi_{i'}(\vec{x})u_{v'}(\vec{\xi})\alpha_i^{v\dagger}\alpha_{i'}^{v'}\ . \tag{20}$$

The operator $\alpha_i^{v\dagger}$ thus creates a molecule in the ith surface state and vth vibrational excitation. The residual Hamiltonian couples the approximate (i,v) states together and will be treated later as a dynamical perturbation.

III. DYNAMICS OF THE GAS-SOLID SYSTEM

A. Laser coupling

We can include the effect of laser radiation in the Hamiltonian using minimal coupling. Denoting the charge acquired by parts A and B in the molecule by $-Q$ and $+Q$, respectively (see Fig. 1), we replace the kinetic energy terms $(-\hbar^2/2m_A)(\partial^2/\partial\vec{x}_A^{\,2})$ and $(-\hbar^2/2m_B)(\partial^2/\partial\vec{x}_B^{\,2})$ in the gas-solid Hamiltonian by

$$-\frac{\hbar^2}{2m_A}\frac{\partial^2}{\partial\vec{x}_A^{\,2}}+\frac{\hbar}{i}Q\frac{1}{m_A}\vec{A}(\vec{x}_A,t)\cdot\frac{\partial}{\partial\vec{x}_A}$$

and

$$-\frac{\hbar^2}{2m_B}\frac{\partial^2}{\partial\vec{x}_B^{\,2}}+\frac{\hbar}{i}Q\frac{1}{m_B}\vec{A}(\vec{x}_B,t)\cdot\frac{\partial}{\partial\vec{x}_B}\ .$$

We then get as part of $H_{\rm dyn}$ in (1) the gas-laser coupling

$$H_{g-l}=-\frac{\hbar}{i}Q\left\{\left[\frac{1}{m_A}\vec{A}\left[\vec{x}-\frac{\mu}{m_A}\vec{\xi},t\right]+\frac{1}{m_B}\vec{A}\left[\vec{x}+\frac{\mu}{m_B}\vec{\xi},t\right]\right]\cdot\frac{\partial}{\partial\vec{\xi}}+\frac{1}{m}\left[\vec{A}\left[\vec{x}-\frac{\mu}{m_A}\vec{\xi},t\right]-\vec{A}\left[\vec{x}+\frac{\mu}{m_B}\vec{\xi},t\right]\cdot\frac{\partial}{\partial\vec{x}}\right]\right\}\ , \tag{21}$$

where we adopted the radiation gauge $\vec{\nabla}\cdot\vec{A}=0$.

The bound-state wave functions for the atoms in the adsorbed molecule all vanish within a few angstroms of the metal surface, while the radiation which couples to the molecular modes has wavelengths exceeding 10^4 Å. We may therefore safely neglect the $\vec{\xi}$ dependence in $\vec{A}$ and get

$$H_{g-l}=-\frac{\hbar}{i}\frac{Q}{\mu}\vec{A}(\vec{x},t)\cdot\frac{\partial}{\partial\vec{\xi}}\ . \tag{22}$$

Introducing the second quantization, and using the expansions for the field operators given by Eq. (17), we get

$$\hat{H}_{g-l}=-\frac{\hbar}{i}\frac{Q}{\mu}\sum_{\substack{i,i'\\ v,v'}}\int\phi_i^*(\vec{x})\vec{A}(\vec{x},t)\phi_{i'}(\vec{x})\,d\vec{x}\cdot\int d\vec{\xi}\,u_v^*(\vec{\xi})\frac{\partial}{\partial\vec{\xi}}u_{v'}(\vec{\xi})\alpha_i^{v\dagger}\alpha_{i'}^{v'}\,. \tag{23}$$

For infrared and visible radiation $\vec{A}(\vec{x},t)$ changes little over the size of the molecule so that $\vec{A}(\vec{x},t)\approx\vec{A}(\vec{0},t)$ where the origin is taken at the adsorption site. We then get from (23)

$$\hat{H}_{g-l}=-\frac{\hbar}{i}\frac{Q}{\mu}\vec{A}(\vec{0},t)\cdot\sum_{i,v,v'}\int d\vec{\xi}\,u_v^*(\vec{\xi})\frac{\partial}{\partial\vec{\xi}}u_{v'}(\vec{\xi})\alpha_i^{v\dagger}\alpha_i^{v'}\,. \tag{24}$$

To go further we must specify the vector potential $\vec{A}(\vec{0},t)$ of the laser at the surface of the solid. In second quantized form it can be written

$$\vec{A}(\vec{0},t)=\left[\frac{\hbar}{2\epsilon_0}\right]^{1/2}\sum_{\vec{K},\Pi}\int_{-\infty}^{0}d\kappa\,\Omega^{-1/2}(\vec{K},\kappa)\{\vec{U}_{\vec{K},\kappa}^{(\Pi)}(0)\exp[-i\Omega(\vec{K},\kappa)t]c_{\vec{K},\kappa}^{(\Pi)}+\text{H.c.}\}\,, \tag{25}$$

where $\vec{K}$ is the component of the wave vector of the incident light along the surface, κ is its component perpendicular to the surface, and Π labels the two possible polarizations. Of course, $\Omega(\vec{K},\kappa)=c(K^2+\kappa^2)^{1/2}$, ϵ_0 is the dielectric constant of vacuum, and $c_{\vec{K},\kappa}^{(\Pi)+}$ creates a photon. The free-laser-field Hamiltonian is thus given by

$$\hat{H}_l=\sum_{\vec{K},\Pi}\int_{-\infty}^{0}d\kappa\,\hbar\Omega(\vec{K},\kappa)(c_{\vec{K},k}^{(\Pi)\dagger}c_{\vec{K},\kappa}^{(\Pi)}+\tfrac{1}{2})\,. \tag{26}$$

The eigenmodes $\vec{U}_{\vec{K},\kappa}^{(\Pi)}(\vec{x})$ of the electromagnetic field must satisfy the appropriate boundary conditions and are given in the Appendix.

B. Phonon coupling

We next consider the internal degrees of freedom of the solid, i.e., the lattice vibrations, in the Hamiltonian (1). In the harmonic approximation we have

$$\hat{H}_p=\sum_J\hbar\omega_J b_J^\dagger b_J\,, \tag{27}$$

where $b_J^\dagger$ creates a phonon of mode J. For simplicity we use a Debye bulk model though the theory can be carried through for proper surface phonon modes as well.[20] To include the effect of the lattice vibrations on the adsorbed molecule we replace in (2),

$$\begin{aligned}V_s^{(A)}(\vec{x}_A)+V_s^{(B)}(\vec{x}_B)&\rightarrow V_s^{(A)}(\vec{x}_A-\vec{u}(t))+V_s^{(B)}(\vec{x}_B-\vec{u}(t))\\&\approx V_s^{(A)}(\vec{x}_A)+V_s^{(B)}(\vec{x}_B)-\vec{u}(t)\cdot\frac{\partial}{\partial\vec{x}}[V_s^{(A)}(\vec{x}_A)+V_s^{(B)}(\vec{x}_B)]\,,\end{aligned} \tag{28}$$

where the last line is obtained in the harmonic approximation. We expand the lattice displacement at the surface

$$\vec{u}(t)=\left[\frac{\hbar}{2\rho}\right]^{1/2}\sum_J\omega_J^{-1/2}[b_J(t)\vec{u}^{(J)}(0)+b_J^\dagger(t)u^{(J)*}(0)]\,, \tag{29}$$

where ρ is the mass density of the solid. The functions $\vec{u}^{(J)}$ ($\vec{r}=0$) have to satisfy proper boundary conditions. In the bulk Debye model they are simply

$$\vec{u}^{(J)}(\vec{0})=\vec{e}_{\vec{p}\sigma}/V_s^{1/2}\,, \tag{30}$$

where $\vec{e}_{\vec{p}\sigma}$ is the polarization vector of a phonon of momentum $\vec{p}$ with σ enumerating transverse and longitudinal modes. The solid occupies a volume V_s and has N_s constituents of mass M_s.

With (17) we get from (28) a contribution to the dynamic part in (1):

$$\begin{aligned}\hat{H}_{g-s}=-\left[\frac{\hbar}{2M_sN_s}\right]^{1/2}\sum_{\vec{p},\sigma}(\omega_{\vec{p}\sigma})^{-1/2}\vec{e}_{p\sigma}\cdot\sum_{\substack{i,i'\\ v,v'}}\int d\vec{\xi}\,d\vec{x}\,\phi_i^*(\vec{x})u_v^*(\vec{\xi})\frac{\partial}{\partial\vec{x}}\left[V_s^{(A)}\left[\vec{x}-\frac{\mu}{m_A}\vec{\xi}\right]+V_s^{(B)}\left[\vec{x}+\frac{\mu}{m_B}\vec{\xi}\right]\right]\\\times\phi_{i'}(\vec{x})u_{v'}(\vec{\xi})\alpha_i^{v\dagger}(b_{\vec{p}\sigma}^\dagger+b_{\vec{p}\sigma})\alpha_{i'}^{v'}\,.\end{aligned} \tag{31}$$

The total Hamiltonian is then given with (18), (24), (26), (27), and (31) by

$$\hat{H}=\hat{H}_g^{(0)}+\hat{H}_l+\hat{H}_s+\hat{H}_{g-l}+\hat{H}_{g-s}+\hat{H}_{\rm res} \ . \tag{32}$$

It will be the basis of the kinetic theory of photodesorption.

IV. KINETICS

We assume that the kinetics of the gas-solid system coupled to the laser field is a stationary Markov process and is controlled by a master equation,

$$\frac{dn_i^v(t)}{dt}=\sum_{i',v'}R_{ii'}^{vv'}n_{i'}^{v'}-\sum_{i',v'}R_{i'i}^{v'v}n_i^v \ , \tag{33}$$

for the occupation functions n_i^v of a state (i,v) of the molecule. Its adequacy for desorption kinetics has been discussed and tested, e.g., in Refs. 7, 21, 27, and 28. The label i enumerates the bound states (i.e., adsorbed molecules) and the continuum states (i.e., gas phase). The transition probabilities R are calculated according to Fermi's golden rule from (32) with $(\hat{H}_g^{(0)}+\hat{H}_l+\hat{H}_s)$ as the unperturbed part.

A. Laser transition probabilities

The contribution from $\hat{H}_{g-l}$ to R is from (24) and (25)

$$\mathscr{L}_{ii'}^{vv'}=\delta_{ii'}\frac{\pi}{\epsilon_0 c}\left[\frac{Q}{\mu}\right]^2\sum_{\vec{K},\Pi}\int_{-\infty}^{0}d\kappa\,(K^2+\kappa^2)^{-1/2}$$
$$\times\left|\int d\vec{\xi}\,u_v^*(\vec{\xi})\frac{\partial}{\partial\vec{\xi}}u_{v'}(\vec{\xi})\cdot\vec{U}_{\vec{K},\kappa}^{(\Pi)}(0)\right|^2$$
$$\times\{n_{\rm em}(\vec{K},\kappa,\Pi)\delta[E_i^v-E_{i'}^{v'}-\hbar c(K^2+\kappa^2)^{1/2}]$$
$$+[n_{\rm em}(\vec{K},\kappa,\Pi)+1]\delta[E_i^v-E_{i'}^{v'}+\hbar c(K^2+\kappa^2)^{1/2}]\} \ , \tag{34}$$

where $n_{\rm em}(\vec{K},\kappa,\Pi)$ is the occupation number of photons of momentum $(\vec{K},\kappa)$ and polarization Π. The integral over $\vec{\xi}$ in (34) is easily computed for harmonic-oscillator wave functions. For further evaluation we now assume that the solid is a dielectric with refractive index n_r. We restrict ourselves to situations where the molecular dipole is perpendicular to the surface so that only light polarized in the plane of incidence ($\Pi=p$) can excite it (for arbitrary orientation see the Appendix). With the eigenfunctions $\vec{U}$ given in the Appendix we then get after replacing the summation over $\vec{K}$ by an integration

$$\mathscr{L}_{ii'}^{vv'}=\delta_{ii'}(Q^2/4\pi^2\epsilon_0\mu c)$$
$$\times\int d^2K\,d\kappa\,K^2n_r^2(K^2+\kappa^2)^{-1}\left[n_r^2+a^2+\frac{2a}{n_r}\right]^{-1}$$
$$\times\{n_{\rm em}(\vec{K},\kappa,\Pi=p)v\delta_{v',v-1}+[n_{\rm em}(\vec{K},\kappa,\Pi=p)+1](v+1)\delta_{v',v+1}\}\,\delta[\Omega/c-(K^2+\kappa^2)^{1/2}] \ , \tag{35}$$

where

$$a=\cos\theta_t/\cos\theta_i \ , \tag{36}$$

where θ_i is the angle between the incident laser beam and the normal, i.e., $\tan\theta_i=|\kappa|/|\vec{K}|$, and θ_t is the angle of the transmitted beam.

Next we must relate the photon occupation numbers

$$n_{\rm em}(\vec{K},\kappa,\Pi)=\langle c_{\vec{K},\kappa}^{(\Pi)\dagger}c_{\vec{K},\kappa}^{(\Pi)}\rangle \ , \tag{37}$$

with the intensity of the incident laser beam in that particular mode. We recall that the intensity of the incoming laser beam is given by

$$I_0=\frac{\sqrt{\epsilon_0}}{\mu_0}\,|\,{}^{\rm in}\vec{\mathrm{E}}^{\,2}(x,t)\,|_{\rm av} \tag{38}$$

averaged over one period. The prefix "in" denotes the fact that in $\vec{\mathrm{E}}(\vec{\mathrm{x}},t)$ we should only keep the incoming field. With an expansion like (25) for $\vec{\mathrm{E}}(\vec{\mathrm{x}},t)$ we get immediately

$$\begin{aligned}I_0&=\sum_{\vec{\mathrm{K}},\Pi}\int_{-\infty}^{0}d\kappa I(\vec{\mathrm{K}},\kappa,\Pi)\\&=c\sum_{\vec{\mathrm{K}},\Pi}\int_{-\infty}^{0}d\kappa\,|\,{}^{\rm in}\vec{\mathrm{U}}^{(\Pi)}_{\vec{\mathrm{K}},\kappa}(\vec{\mathrm{x}})\,|^2\hbar c(K^2+\kappa^2)^{1/2}\\&\quad\times[n_{\rm em}(\vec{\mathrm{K}},\kappa,\Pi)+\tfrac{1}{2}]\,.\end{aligned} \tag{39}$$

From (A3) we get for p waves

$$|\,{}^{\rm in}\vec{\mathrm{U}}^{(\Pi=p)}_{\vec{\mathrm{K}}\kappa}(\vec{\mathrm{x}})\,|^2=\frac{1}{2\pi L^2}\frac{(n_r+a)^2}{n_r^2+a^2+2a/n_r} \tag{40}$$

where L^2 is the area of the surface. We also go to the continuous limit in (35) by the replacement

$$\sum_{\vec{\mathrm{K}}}\rightarrow(L/2\pi)^2\int d^2K\,. \tag{41}$$

Finally we specify that the laser is perfectly collimated along the incident beam direction and has a Lorentzian frequency distribution around Ω_l of width Γ_l. This then allows us to identify the occupation functions as follows

$$n_{\rm em}(\vec{\mathrm{K}},\kappa,\Pi=p)+\tfrac{1}{2}=I_0\frac{(2\pi)^3c^2}{(\hbar\Omega^{13})}\frac{n_r^2+a^2+2a/n_r}{(n_r+a)^2}$$

$$\times\delta(\phi-\phi_i)\delta(\cos\theta-\cos\theta_i)(\Gamma_l/2\pi)[(\Omega'-\Omega_l)^2+\Gamma_l^2/4]^{-1}\,, \tag{42}$$

where $\Omega'=c(K^2+\kappa^2)^{1/2}$ and I_0 is the intensity of the incoming beam far from the surface. Before we use (42) to evaluate (35), a few clarifying remarks are necessary. We have set up the Hamiltonian (32) with the vibrational degree of freedom of the molecule represented by a harmonic oscillator. Energy conservation in vibrational transitions then produces the δ function in (35). To avoid infinities we must then give a linewidth Γ_l to the laser. This is, indeed, reasonable for the description of typical laser-induced desorption experiments in which pulsed lasers are used of pulse length typically $\tau_l=2\times10^{-7}$ s, i.e., of width $\Gamma_l=\tau_l^{-1}=5\times10^6$ s^{-1}. We will see in Sec. V from our numerical work that the width of the vibrational levels of the molecule, produced by the coupling $\hat{H}_{g-s}$ and $\hat{H}_{\rm res}$ in (32) is typically 10^9-10^{11} s^{-1}, i.e., many orders larger than the laser width Γ_l and also much larger than its inherent linewidth Γ_m due to the coupling of the vibrational levels to electromagnetic vacuum fluctuations. With a continuous laser of very small bandwidth, typically of the order 10 s^{-1}, some caution is necessary, as the inherent linewidth of the vibrational transitions of the molecule $\Gamma_m\approx10^3$ s^{-1} is definitely larger than that. It is then advisable to replace the δ function in (35) by a Lorentzian of width Γ_m and treat the laser as monochromatic, i.e., let Γ_l go to zero as done, e.g., by Jedrzejek *et al.*[7] For a (pulsed) laser of width $\Gamma_l\gg\Gamma_m$ we get from (35), using (42)

$$\mathscr{L}^{vv'}_{ii'}=2\pi Q^2(\epsilon_0\mu c\hbar\Omega_l)^{-1}n_r^2\sin^2\theta_i\{n_r+[1+(1-n_r^{-2})\tan^2\theta_i]^{1/2}\}^{-2}(2I_0\tau_l/\pi)[v\delta_{v',v-1}+(v+1)\delta_{v',v+1}]\delta_{ii'}\,. \tag{43}$$

Note that $I_0\tau_l=F_l$ is the (approximate) fluence of the laser pulse.

B. Phonon-transition probabilities

The contribution to the transition probabilities R in (33) from $\hat{H}_{g-s}$ in (31) is

$$\begin{aligned}P^{vv'}_{ii'}=\frac{\pi}{M_sN_s}\sum_{\vec{\mathrm{p}},\sigma}\omega^{-1}_{\vec{\mathrm{p}}\sigma}\{&n_{\rm ph}(\omega_{\vec{\mathrm{p}}\sigma})\delta(E_i^v-E_{i'}^{v'}-\hbar\omega_{\vec{\mathrm{p}}\sigma})+[n_{\rm ph}(\omega_{\vec{\mathrm{p}}\sigma})+1]\delta(E_i^v-E_{i'}^{v'}+\hbar\omega_{\vec{\mathrm{p}}\sigma})\}\\&\times\left|\vec{\epsilon}_{\vec{\mathrm{p}}\sigma}\cdot\int d\vec{\mathrm{x}}\,d\vec{\xi}\,\phi_i^*(\vec{\mathrm{x}})u_v^*(\vec{\xi})\frac{\vec{\partial}}{\partial\vec{\mathrm{x}}}\left[V_s^{(A)}\left[\vec{\mathrm{x}}-\frac{\mu}{m_A}\vec{\xi}\right]+V_s^{(B)}\left[\vec{\mathrm{x}}+\frac{\mu}{m_B}\vec{\xi}\right]\right]u_{v'}(\vec{\xi})\phi_{i'}(\vec{\mathrm{x}})\right|^2,\end{aligned} \tag{44}$$

where $n_{\rm ph}(\omega)$ is the Bose-Einstein occupation function for phonons. To evaluate the $\vec{\xi}$ integrals we do a Taylor expansion of the V_s in terms of $(\xi-\xi_0)\vec{n}$, where $\vec{n}$ is a unit vector along the molecular dipole axis, i.e., perpendicular to the surface, leading to integrals of the type

$$\int d\xi\, u_v^*(\xi)(\xi-\xi_0)^l u_{v'}(\xi)\ , \tag{45}$$

between shifted harmonic-oscillator states which can be easily computed.

For the following calculations we choose the surface potential to be a one-dimensional Morse potential for which the wave functions $\phi_i(z)$ are known explicitly. One could keep the theory three dimensional and the surface potential more realistic like sums of Lennard-Jones potentials; however, this would imply extensive numerical work (which we have shown in previous work[20] to be manageable); we therefore prefer here a simpler and analytic approach. One can show numerically that in (44) as well as in $\hat{H}_g^{(0)}$ in (32) one can safely drop the $V_s^{(B)}$ term. Then the $\vec{x}$ integrals in (44) are of the same structure as those appearing in the cascade model of thermal desorption.[21] We therefore just quote the final result after introducing dimensionless variables

$$\begin{aligned}
&\sigma_0^2=2mV_0/(\hbar\gamma)^2\ ,\\
&r=2m\omega_D/\hbar\gamma^2\ ,\\
&\delta=\hbar\omega_D/k_BT\ ,\\
&\Delta=\Omega/\omega_D\ ,\\
&\epsilon_i^v=E_i^v/\hbar\omega_D\\
&\quad=-r^{-1}(\sigma_0-i-\tfrac{1}{2})^2+(v+\tfrac{1}{2})\Delta\ ,
\end{aligned} \tag{46}$$

where ω_D is the Debye frequency; V_0 and γ are depth and inverse range of the Morse potential. For bound-state–bound-state transitions we have

$$\begin{aligned}
P_{ii'}^{vv'}=&\omega_D(\epsilon_i^v-\epsilon_{i'}^{v'})\{\exp[\delta(\epsilon_i^v-\epsilon_{i'}^{v'})]-1\}^{-1}\,\Theta(1-|\epsilon_i^v-\epsilon_{i'}^{v'}|)24\pi\sigma_0^2r^{-3}(m/M_s)(v_>!/v_<!)(|v-v'|!)^2\\
&\times\left[\frac{4m_B}{m_Ar\Delta}\right]^{|v-v'|}(i-i')^2\,(\sigma_0-i-\tfrac{1}{2})(\sigma_0-i'-\tfrac{1}{2})(i_>!/i_<!)\left[\frac{2\sigma_0-i-i'-1}{2\sigma_0}+\frac{1-2^{-|v'-v|}}{|i-i'|}\right]^2\\
&\times\Gamma(2\sigma_0-i_>)/\Gamma(2\sigma_0-i_<)\ ,
\end{aligned} \tag{47}$$

where $i_<$ and $i_>$ are the smaller or larger of i and i'. For $(\epsilon_i^v-\epsilon_{i'}^{v'})>0$ the transition occurs via absorption of a phonon; otherwise via stimulated and spontaneous emission. For $v=v'$ (47) reduces to the expression in the phonon cascade model.[21]

To describe desorption with the master equation (33) we must also know all transitions from any (i',v') bound state into all accessible continuum states with vibrational quantum number v. It is given by

$$\begin{aligned}
P_{ci'}^{vv'}=&\omega_D(3\pi/4)(m/M_s)(v_>!/v_<!)(|v-v'|!)^{-2}(4m_B/m_Ar\Delta)^{|v-v'|}\\
&\times\frac{2\sigma_0-2i'-1}{i'!\Gamma(2\sigma_0-i')}\int_{\epsilon_{i'}^{v'}-v\Delta-1}^{\epsilon_{i'}^{v'}+v\Delta+1}dx\,\Theta(x)(x-\epsilon_{i'}^{v'}+v\Delta)\\
&\times\{\exp[\delta(x-\epsilon_{i'}^{v'}+v\Delta)]-1\}^{-1}\,|\Gamma(\sigma_0+\tfrac{1}{2}+i\sqrt{rx})|^2\frac{\sinh(2\pi\sqrt{rx})}{\cos^2(\pi\sigma_0)+\sinh^2(\pi\sqrt{rx})}\\
&\times\left[x+\frac{(\sigma_0-i'-\frac{1}{2})^2+2\sigma_0(1-2^{-|v-v'|}}{r}\right]^2.
\end{aligned} \tag{48}$$

(The argument of the Γ function is complex, i.e., $i=\sqrt{-1}$.) Again for $v=v'$ this reduces to the known result.[21]

C. Transition probabilities due to the residual interaction.

Transitions due to the residual interaction (20) are due to tunneling between states of $H_g^{(0)}$ and are not aided by either phonon or photon fields. They are the ones considered by Lucas and Ewing[9] in their model of vibrational predissociation. Because the energies of initial and final states must be the same for such tunneling these transitions can take place only in the continuum, apart from some rather unlikely situations. The transition probability summed over all available continuum states is given by Fermi's golden rule as (neglecting again $V_s^{(B)}$)

$$Q_{ci'}^{vv'}=\frac{2\pi}{\hbar}\sum_{\vec{q}}\left|\int d\vec{x}\,d\vec{\xi}\,\phi_{\vec{q}}^{*}(\vec{x})u_v^{*}(\vec{\xi})\left[V_s^{(A)}\left[\vec{x}-\frac{\mu}{m_A}\vec{\xi}\right]-V_s^{(A)}\left[\vec{x}-\frac{\mu}{m_A}\vec{\xi}_0\right]\right]\phi_{i'}(\vec{x})u_{v'}(\vec{\xi})\right|^2\delta(E_{\vec{q}}^{v}-E_{i'}^{v'}) , \tag{49}$$

where $\vec{q}$ is the center-of-mass wave number of a molecule in the continuum of energy $\hbar^2q^2/2m$. Again we expand the potential in a Taylor series in $(\xi-\xi_0)\vec{n}$ and obtain in the dimensionless variables (46)

$$Q_{ci'}^{vv'}=\omega_D(r\pi/16)(v_>!/v_<!)(|v-v'|!)^{-2}\times\left[\frac{4m_B}{m_Ar\Delta}\right]^{|v-v'|}\frac{2\sigma_0-2i'-1}{i'!\Gamma(2\sigma_0-i')}$$
$$\times|\Gamma[\sigma_0+\tfrac{1}{2}+i\sqrt{r(\epsilon_{i'}^{v'}-v\Delta)}]|^2\frac{\sinh[2\pi\sqrt{r(\epsilon_{i'}^{v'}-v\Delta)}]}{\cos^2(\pi\sigma_0)+\sinh^2[\pi\sqrt{r(\epsilon_{i'}^{v'}-v\Delta)}]}$$
$$\times[(v'-v)\Delta+\frac{2\sigma_0}{r}(1-2^{1-|v-v'|})]^2\Theta(\epsilon_{i'}^{v'}-v\Delta) . \tag{50}$$

For σ_0 an integer, $v=0$, $v'=1$, and in the limit $r\,\epsilon_{i'}^{v'}\to\infty$ (50) reduces to the expression given by Lucas and Ewing,[9] their equation (9).

D. The master equation

To describe photodesorption with the master equation (33) we drop the transitions from the continuum back to the bound states (appropriate for an experiment in which the gas phase is pumped out during the laser irradiation). We then get for the occupation of the bound states

$$\frac{dn_i^v(t)}{dt}=\sum_{v'=0}^{\infty}\sum_{i'=0}^{i_{\max}}[(\mathscr{L}_{ii'}^{vv'}+P_{ii'}^{vv'})n_{i'}^{v'}(t)-(\mathscr{L}_{i'i}^{v'v}+P_{i'i}^{vv'})n_i^v(t)]$$
$$-\sum_{v'=0}^{\infty}(P_{ci}^{v'v}+Q_{ci}^{v'v})n_i^v(t) , \tag{51}$$

where $(i_{\max}+1)$ is the number of bound states in the Morse potential, determined as the maximum integer such that $\sigma_0-i_{\max}-\frac{1}{2}>0$.

After calculating the transition probabilities P, $\mathscr{L}$, and Q we have solved (51) by matrix diagonalization (after truncating the summation over the vibrational quantum number v) starting from an initial thermal occupation

$$n_i^v(t=0)=A\exp(-\delta\epsilon_i^v) . \tag{52}$$

The total occupation in the adsorbate then develops according to

$$N(t)/N(0)=\frac{\sum_{v=0}^{\infty}\sum_{i=0}^{i_{\max}}n_i^v(t)}{\sum_{i',v'}n_{i'}^{v'}(0)}=\sum_j S_je^{-\lambda_jt} , \tag{53}$$

where $(-\lambda_j)$ are the eigenvalues of the matrix $(\mathscr{L}+P+Q)$ in (51). In most cases one finds that the lowest eigenvalue λ_0 is much smaller than all other λ_j, $j>0$, and contributes to the sum (53) with the largest weight $S_0\approx1$ with $S_j\ll S_0$. Thus the evolution of the total occupation in desorption experiment is controlled by a single time scale λ_0 which can be identified as the rate of desorption $r_d=\lambda_0$ or the desorption time $t_d=\lambda_0^{-1}$. Details of the calculational methods are discussed at great length in Refs. 21, 27, and 28.

V. RESULTS

Before we present numerical results on the photodesorption rates in particular systems we would like to discuss the structure of the master equation (51) and relate it to the schematics of Fig. 1. Let us first set all transition probabilities P and Q equal to zero and only keep $\mathscr{L}_{ii}^{vv'}\neq0$. Equation (51) then has a steady-state population in which, for a given i, all v levels are equally occupied. If the gas-solid system was initially, i.e., before the laser was switched on, in equilibrium then the steady-state occupation is simply

$$n_i^v=A\,e^{-\beta E_i} , \tag{54}$$

where E_i is an energy eigenvalue of H_m, see (15), and A is a normalization constant. In our theory the molecular vibrations are modeled by a harmonic oscillator (quantum number v). This, of course, is only reasonable up to a certain $v_{\max}$, above which anharmonic frequency shifts and linewidth can no longer be neglected. We will therefore, in our numerical work, truncate the harmonic oscillator at some $v_{\max}$, studying, of course, the dependence of the photodesorption rates as a function of $v_{\max}$.

Let us next switch on, in addition to $\mathscr{L}_{ii}^{vv'}$ the transition probabilities $(P_{ci}^{vv'}+Q_{ci}^{vv'})$ in the master

equation (51) that causes transitions to continuum states, i.e., that desorb molecules. Because all bound-state transitions are still suppressed ($P_{ii'}^{vv'}=0$) desorption can, for the system depicted in Fig. 1, proceed as follows: We assume that at times $t \leq 0$ the gas-solid system is in thermal equilibrium with the laser switch off. The energy levels E_i^v are then thermally occupied

$$n_i^v(t \leq 0) = A\, e^{-\beta E_i^v} . \tag{55}$$

At time $t=0$ the laser is switched on; its itensity is I_0 and, if pulsed of duration τ_l, delivers a fluence $F_l = I_0 \tau_l$. In our theory we also assume that the gas phase is removed, so that we may, for $t>0$, set the occupation of the continuum states equal to zero. The experiments on the CH_3F-NaCl system by Heidberg *et al.*[11–13] are done at $T=77$ K where thermal desorption is negligible (the heat of adsorption is about 3000 K) and the pressure above the surface is about 10^{-9} mbar, justifying the above procedure. Let us in the following discussion (not, however, in the numerical work) assume that only the ground state $i=v=0$ is initially occupied. Switching on the laser will then take a molecule from a state $(i,v)=(0,0)\rightarrow(0,1)\rightarrow(0,2)\rightarrow\cdots\rightarrow(0,v_{\max})$ with a transition probability typically of order $\mathcal{L}_{ii}^{vv\pm1}=10^9 F_l$, see (43). Let us for the system depicted in Fig. 1 first set $v_{\max}=2$. At very low fluence such that $(P_{c0}^{02}+Q_{c0}^{02}) \gg \mathcal{L}_{00}^{02}$ all molecules pumped up to $v=2$ will desorb so that the overall desorption rate r_d is controlled by the bottleneck of the laser, so that r_d is linear in F_l. Increasing the fluence will eventually lead to a situation where $(P_{c0}^{02}+Q_{c0}^{02}) \ll \mathcal{L}_{00}^{02}$ so that now the bottleneck exists at the top and the rate becomes independent of F_l, i.e., we have saturation. If we now increase $v_{\max}$, the rate will increase because more desorption channels open, e.g., due to $(P_{c0}^{13}+Q_{c0}^{13})$ and $(P_{c0}^{03}+Q_{c0}^{03})$. Note from expressions (48) and (50) that

$$\begin{aligned} \frac{P_{c0}^{13}+Q_{c0}^{13}}{P_{c0}^{02}+Q_{c0}^{02}} &= \frac{3!}{2!} = 3 , \\ \frac{P_{c0}^{03}+Q_{c0}^{03}}{P_{c0}^{02}+Q_{c0}^{02}} &= \frac{3!}{2!} = 3 , \end{aligned} \tag{56}$$

so that desorption rates in the saturation range increase significantly with $v_{\max}$; still with all phonon cascades, i.e., bound-state–bound-state transitions $P_{ii'}^{vv'}$ suppressed. We next include the latter in the master equation (51). Even without a laser, molecules can now desorb thermally in a cascade of many one-phonon processes mainly due to $P_{ii'}^{00}$ and P_{ci}^{00} as in the cascade model.[21] With the laser on we can now also have the following process: $(i,v)=(0,0)\rightarrow(0,1)\rightarrow(i_0,0)$; from the latter state a quick cascade of one-phonon emission processes with transition probabilities typically of the order $10^{14}-10^{15}$ s^{-1} will bring the molecule back to the ground state $(i,v)=(0,0)$; thus transforming the initial laser photon of energy $\hbar\Omega$ into many phonons: We called this process resonant heating. This is obviously a loss process as far as desorption goes and should reduce the desorption rate. It also produces the significant linewidth of the vibrations of adsorbed molecules. In addition to the loss mechanism $(i,v)=(0,0)\rightarrow(0,1)\rightarrow(i_0,0)\rightarrow(0,0)$ we can also desorb via $(0,0)\rightarrow(0,1)\rightarrow(i_0,0)\rightarrow$(cont., 0) where the last step in the second process thermally desorbs the molecule from the state $(i_0,0)$ with an activation energy that is only half the depth of the surface potential. This process should therefore be much faster than thermal desorption from the ground state if it dominates over the downward cascade $(i_0,0)\rightarrow(0,0)$ which it does only at high temperatures.

The laser will also pump the molecule through a sequence $(i,v)=(0,0)\rightarrow(0,1)\rightarrow(0,2)$ after which desorption occurs via $(P_{c0}^{02}+Q_{c0}^{02})$. From $(i,v)=(0,2)$ we can also go in a phonon-mediated process $P_{i^*0}^{12}$ to $(i^*,1)$, then desorb, or cascade down to (0,1), tunnel into $(i_0,0)$, and cascade down to (0,0). In most systems, the additional desorption channels will dominate the loss (heating) mechanisms so that with increasing $v_{\max}$, the desorption rate will rise. For a fixed $v_{\max}$, large fluences F_l will again lead to saturation.

To substantiate this discussion we have evaluated the above theory of photodesorption numerically for two systems, namely CH_3F and CO on NaCl, calcu-

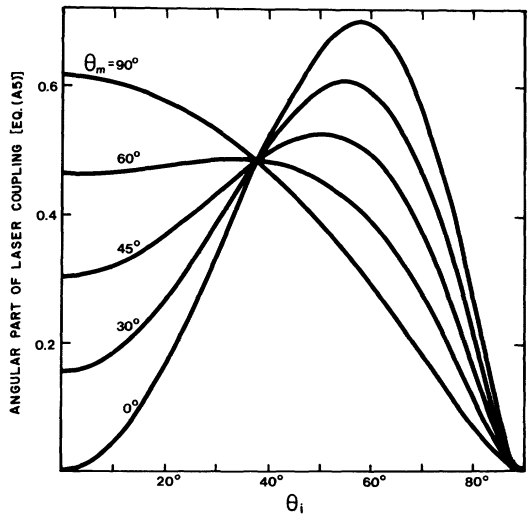

FIG. 2. The angular part of the laser coupling (A5) with $I_{\rm inc}^{(p)}/I_{\rm inc}^{(s)}=1$ as a function of the angle of laser incidence θ_i with respect to the normal, with θ_m the orientation of the molecule (averaged over polar orientation).

lating desorption rates by solving the master equation as outlined at the end of Sec. IV and detailed, e.g., in Ref. 21. The parameters entering the theory are the masses m_A and m_B and effective charge Q of the constituents A and B of the molecule, the vibrational frequency Ω of the active mode, the Debye temperature T_D of the solid ($T_D=281$ K for NaCl), mass of the unit cell of the solid M_s, its refractive index ($n_r=1.544$), and the depth V_0 and range γ^{-1} of the surface Morse potential. Variables are temperature T, laser fluence F_l (or intensity I_0) and angle of incidence θ_i of the laser with respect to the surface normal. Changing the angle of incidence alters the local electric and magnetic fields in the vicinity of the adsorbed molecule and thus the coupling into its dipole $\vec{\mu}$. This is depicted in Fig. 2 where we plot $(\vec{E}\cdot\vec{\mu})^2$ as a function of θ_i. All subsequent calculations of desorption rates are done for an angle $\theta_i=60°$ of optimal coupling. Rates at other angles of laser incidence can be deduced with the help of Fig. 2 by enhancing or reducing the fluence values given accordingly.

A. CH_3F on NaCl

The two parts A and B of CH_3F are identified as F and the CH_3 radical, respectively, with mass numbers $m_A=19$ and $m_B=15$. There is no evidence in what position CH_3F is adsorbed on NaCl though one can speculate[22] from electronegativity and size that F is sitting over Na. For our theory this is not crucial because of the small mass difference between m_A and m_B. For the free CH_3F molecule the derivative of the dipole moment is[23] $\partial\mu/\partial\xi=4.6$ debye/Å implying an effective charge $Q=qe\approx e$, i.e., $q\approx 1$. Most molecules, however, change their dipole moment significantly upon adsorption on a solid. Unfortunately, nothing seems to be known about the dipole moment of adsorbed CH_3F. We therefore take q as determined in the free molecule and keep in mind that q enters the theory only in the combination (q^2F_l) so that a different value of q simply implies a rescaling of the fluence.

The active vibration of CH_3F into which the laser is tuned has a wave number in the free molecule of $\nu_3=1048$ cm^{-1}. Adsorbed on NaCl it is reduced[11] to 970 cm^{-1} so that $\hbar\Omega/k_B=1400$ K. Next we consider the parameters of the surface potential. Its depth V_0 can be equaled to the heat of adsorption measured to be about[11,12] or somewhat less than[22] 25 kJ/mol or 3025 K per particle. From this depth it takes at least three photons of energy $\hbar\Omega$ each to lift the molecule into a state degenerate with the continuum, whereas a reduction of 10% (within the experimental uncertainty) in V_0 to 22.5 kJ/mol would allow this to happen in a two-photon process. Nothing is known about the range γ^{-1} of the surface potential except that it is certainly less than an angstrom. We have therefore studied four potential models differing in depth as indicated above and varying in range from 0.25 to 0.35 Å. We begin with a model with $V_0=2570$ K and $\gamma^{-1}=0.25$ Å so that the dimensionless parameters in (46) are $\sigma_0=16.3$ and $r=27.5$. The surface Morse potential has therefore 16 bound states the lowest two of which are separated by $(E_1-E_0)=2\ (\sigma_0-1)\hbar\omega_D/r \approx 1.11\hbar\omega_D$. Thermal desorption is therefore not possible by one-phonon cascades, as it takes at least the simultaneous absorption of two phonons for a molecule to be lifted from E_0 to E_1. As our theory so far includes only one-phonon processes, some features of this model system are somewhat artificial; they, however, highlight nicely some details of the photodesorption process, which are less obvious in the next system (with $E_1-E_0\approx 0.81\hbar\omega_D$) to be considered.

In Fig. 3 we present the fluence dependence of the desorption rate as calculated from (51) for various temperatures and $v_{\max}$. In a first calculation we truncate the vibrational ladder at $v_{\max}=1$. The laser can then lift the adsorbed molecule only halfway up the surface potential well (see Fig. 1) to a state $(i,v)=(0,1)$ from where phonon-assisted inelastic tunneling will take it to $(i^*,0)$ with a rate of about 10^{11} s^{-1}. Subsequently a very fast cascade with typical transition probabilities $P^{00}_{ii'}\approx 10^{14}$ s^{-1} will take it down into lower bound states of the surface potential, the surplus energy being given off in emitting phonons. As the latter energy-loss mechanism is, in our theory, included in the one-phonon approximation, the downward cascade ends at the state $(i,v)=(2,0)$, because for this model the second excited surface state E_2 is separated from the first excited state E_1 by more than the Debye energy. This is certainly an artifact of the present choice of potential parameters, but is useful, nevertheless, for the study of the overall process: Indeed, one finds that at very low fluence and not too high temperature, desorption is thermally activated, i.e., that the rate can be parametrized according to Arrhenius and Frenkel as

$$r_d=\nu e^{-Q/k_BT}, \tag{57}$$

with a heat of adsorption $Q\approx -E_2$, rather than $(-E_0)$ as one would expect for straight thermal desorption. Increasing fluence will keep some of the higher-surface bound states occupied via the channel $(i,v)=(0,0)\rightarrow(0,1)\rightarrow(i^*,0)\rightarrow(i\geq 2,0)$ so that the effective heat of adsorption is still smaller. If we include more harmonic oscillator states, i.e., set

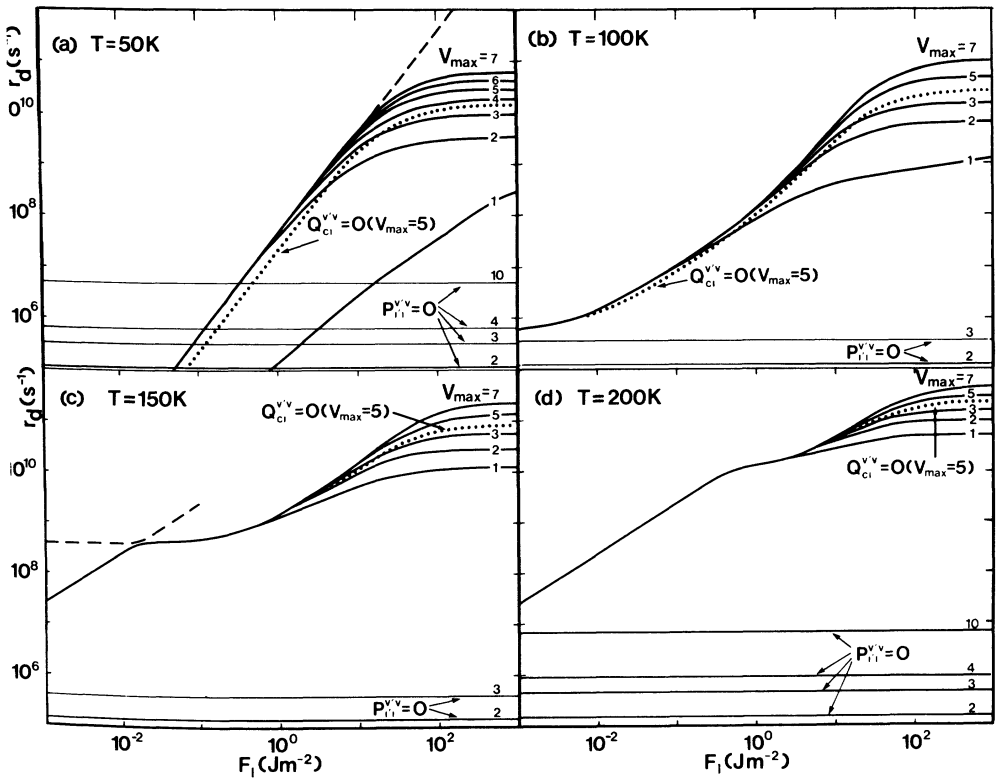

FIG. 3. Photodesorption rate r_d from (51) for CH_3F on NaCl vs laser fluence $F_l=I_0\tau_l$ with I_0 the incident laser intensity and τ_l the duration of laser pulse. v_{max} is the maximum number of oscillator states included for the vibrational mode of CH_3F. Parameters in (46) $\sigma_0=16.3$, $r=27.5$. Dotted line without elastic tunneling, $Q_{ci}^{v'v}=0$, for $v_{max}=5$. Dashed line in (c): third eigenvalue of the transition matrix $(\mathcal{L}+P+Q)$ in (51) as examplified in Table I. Also given are the rates with bound-state–bound-state transitions put equal to zero: $P_{i'i}^{v'v}=0$.

$v_{max}\geq 2$, the desorption rate at $T=50$ K becomes much larger (as compared to $v_{max}=1$) because now a new mechanism takes over in that the laser pumps the molecule into vibrational states degenerate with the continuum, i.e., $(i,0)=(0,0)\rightarrow(0,1)\rightarrow(0,2)\rightarrow(\text{cont.},0)$ where the last step is caused by $(P_{ci}^{vv'}+Q_{ci}^{vv'})$. At low fluences $F_l<1 J m^{-2}$ the rate rises at $T=50$ K and for $v_{max}\geq 2$ like $r_d\sim F_l^{\alpha}$ where $\alpha\approx 2$.

For $F_l>1$ J m^{-2} the rates increase less than quadratically and eventually saturate with asymptotic values depending on v_{max}. This is a consequence of the fact that a high-intensity laser populates all vibrational states up to v_{max} in a very short time so that the desorption rate is limited by the (fluence independent) transition probabilities $(P_{ci}^{vv'}+Q_{ci}^{vv'})$, see the arguments around (56). Indeed, the quadratic power law $r_d\sim F_l^2$ seems to be the asymptotic behavior for large v_{max} though one might expect a slower increase for very large v_{max}. This is, however, a somewhat academic problem, because we should not expect the vibrational levels of the adsorbed CH_3F molecule to be harmonic (as assumed in the theory) for too-large quantum numbers v. Nothing seems to be known about anharmonic effects in adsorbed CH_3F although Heidberg *et al.*[11] argue that $v_{max}\approx 3$ though for different reasons.

To see the importance of the various terms in the master equation (51) we first put the elastic tunneling matrix elements, i.e., $Q_{ci'}^{vv'}$ equal to zero. We recall that this was the process studied by Lucas and Ewing.[9] The rates are down by about a factor of 2 for this system at $T=50$ K for all fluences shown in Fig. 3(a) and also for every v_{max}. With $Q_{ci'}^{vv'}$ switched on again we next suppress all bound state-bound state transitions by putting $P_{ii'}^{vv'}=0$. To start with no desorption is now possible if we restrict $v_{max}=1$. But even when we keep more vibrational states with $v_{max}\geq 2$ desorption is down considerably for all but the lowest fluences because most of the desorption channels depicted in Fig. 1 are now closed, the only available ones being $(i,v)=(0,0)\rightarrow(0,1)\rightarrow(0,2)\rightarrow(\text{cont.},0)$, or $(0,0)\rightarrow(0,1)\rightarrow(0,2)\rightarrow(0,3)\rightarrow(\text{cont.},1)$ and similar ones up to $v=v_{max}$. Note also that with $P_{ii'}^{vv'}=0$, the rates are basically independent of temperature and

TABLE I. Eigenvalues λ_i (s^{-1}) of the matrix $(\mathcal{L}+P+Q)$ and weights S_i in (53) for CH_3F-NaCl at $T=150$ K for the potential parameters of Fig. 3 for $v_{max}=3$. Higher values typically: $\lambda_{32}\approx 2.2\times 10^{14}$, $S_{32}\approx 10^{-17}$, $\lambda_{64}\approx 1.3\times 10^{15}$, and $S_{64}\approx 10^{-21}$.

F_l ($J\,m^{-2}$)	λ_0	S_0	λ_1	S_1	λ_2	S_2	λ_3	S_3
0.002	5.0×10^7	1.1256	5.0×10^7	2.5×10^{-3}	3.9×10^8	−0.1259	1.2×10^{11}	6.3×10^7
0.006	1.5×10^8	1.5798	1.5×10^8	1.8×10^{-4}	3.9×10^8	−0.58	1.2×10^{11}	1.7×10^{-7}
0.01	2.5×10^8	2.5687	2.5×10^8	1.0×10^{-4}	4.0×10^8	−1.5688	1.2×10^{11}	2.5×10^{-7}
0.02	4.0×10^8	4.5498	5.0×10^8	6.5×10^{-5}	5.1×10^8	−3.5497	1.2×10^{11}	$3.1\times^{10}\_7$
0.03	4.1×10^8	2.2053	7.4×10^8	-2.2×10^{-4}	7.5×10^8	−1.2051	1.2×10^{11}	1.9×10^{-7}
0.1	4.9×10^8	1.2451	2.4×10^9	-1.1×10^{-2}	2.5×10^9	−0.2440	1.3×10^{11}	-5.6×10^{-7}
1.0	1.5×10^9	1.0706	2.1×10^{10}	-3.4×10^{-3}	2.2×10^{10}	−0.0658	1.8×10^{11}	-4.5×10^{-7}

fluence, except for very high temperature or very low fluence because $P_{ci'}^{vv'}$ is mostly dominated by spontaneous phonon emitting processes.

Going up to a temperature $T=100$ K increases the rates by about a factor of two but changes little in the qualitative picture, see Fig. 3(b). At $T=150$ K, Fig. 3(c), however, new features appear. First, for fluences $F_l<10^{-2}$ $J\,m^{-2}$ the desorption rate rises linearly with fluence for $v_{max}>2$ because here desorption can occur at most as fast as the vibrational levels degenerate with the continuum are populated. As the fluence is increased beyond 10^{-2} $J\,m^{-2}$, the desorption rate becomes nearly constant to rise again for fluences beyond 1 $J\,m^{-2}$ to eventually saturate at values depending on v_{max}. To understand the origin in the break at $F_l\approx 10^{-2}$ $J\,m^{-2}$, we recall that the solution of the master equation (51) is given by (53) where the λ_i's are the eigenvalues of the complete matrix $R_{ii'}^{vv'}$ of transition probabilities, it so happens that for physically interesting systems, temperatures, and fluences, the smallest eigenvalue λ_0 appears in the sum (53) with the largest weight S_0 so that it can be identified as the desorption rate. All other eigenvalues λ_i, $i>0$ are typically of order $10^{12}-10^{15}$ s^{-1} and appear with extremely small weights S_i in (53) so that they represent small and fast initial transients. In the region of interest, i.e., around $F_l\approx 10^{-2}$ $J\,m^{-2}$, several eigenvalues are of order λ_0 with one having also a weight of order one, as is demonstrated in Table I. This eigenvalue exchanges its role with λ_0 at this particular fluence as indictaed in Fig. 3(c). We should also point out that the matrix $(\mathcal{L}+P+Q)$ in (51) is, in the presence of the laser terms, no longer symmetric, so that pairs of complex eigenvalues are possible. They, indeed, occur at high fluence and temperature with real parts of the order 10^{14} s^{-1} and imaginary parts about 10^{12} s^{-1} appearing with extremely small weights in the sum (53). Increasing temperature to $T=200$ K [Fig. 3(d)] increases the rates slightly but basically follows the same behavior as just discussed at $T=150$ K. The linear rise of r_d for small F_l is identical for $T\geq 150$ K. We should note that thermal desorption (if included in the theory) will, for small fluences, eventually terminate the linear portion as the rate must always be larger than the thermal one. From the temperature dependence of the "flat" eigenvalue we can identify it as being the rate of thermal desorption from the state E_2 (that again is an artifact of the present choice of potential parameters which do not allow one-phonon processes to connect states E_0 with E_1 and E_1 with E_2).

In a second model for the CH_3F-NaCl system we have increased the depth of the surface potential to $V_0/k_B=3025$ K, yielding a heat of adsorption of 25 kJ/mol. With the range $\gamma^{-1}=0.25$ Å the same as in

the previous model, a deeper potential has a large derivative, so that the coupling to the phonons gets stronger. Predictably the rates increase, e.g., by about a factor of 2 at $T=100$ K.

Next we look at a model for the CH_3F-NaCl system in which we increase the range γ^{-1} of the surface potential to 0.35 Å keeping the depth at $V_0/k_B=2750$ K, so that $\sigma_0=22.82$ and $r=53.9$. The CH_3F molecule can now get trapped into 23 bound states the lowest two of which are separated by $E_1-E_0\approx 0.81\hbar\omega_D$. With the laser switched off, thermal desorption by a cascade of one-phonon process is now possible. The rate, calculated from the master equation (51) with fluence $F_l=0$, can be parametrized by the Arrhenius-Frenkel formula (57) with $Q\approx V_0$ and $\nu=2\times 10^{14}$ s^{-1}. We have calculated the fluence dependence of the photodesorption rates from (51) for $T=50$ and 100 K and for various $v_{\max}$, see Fig. 4. At low fluences the photodesorption rate gets slowly larger than the thermal desorption rate; there is around $F_l\sim 10^{-3}$ J m^{-2} an indication of a quadratic rise, i.e., $r_d\sim F_l^2$. At high-fluence saturation is reached earlier and the rates are typically smaller in this model by 5–6 orders of magnitude. Indeed, the loss mechanisms become much more effective, e.g., let us pump, with the laser, a molecule from $(i,v)=(0,0)$ to (0,1). From here it can go to $(i^*,0)$ via inelastic tunneling $P^{01}_{i^*0}$ and cascade down by emission of phonons all the way to the bottom of the potential well to $(i,v)=(0,0)$. Thus the photon does not aid the desorption process. Because in the previous model the downward cascade stopped at $(i,v)=(2,0)$, some of the photon energy could then be saved and used for desorption. Had we included coherent two-phonon processes in our theory (as we will be doing shortly following Ref. 24), the cascade would have continued from (2,0) to (0,0) thus reducing the rates in Fig. 3, to pull them more in line with those in Fig. 4.

For the model parameters yielding Fig. 4 we again looked at the various contributions in the master equation (51). If we set all bound-state–bound-state transitions to zero, $P^{v'v}_{i'i}=0$, the rates are reduced for all fluences shown to about 20 s^{-1} at both temperatures, indicating again the importance of the various cross channels in Fig. 1. Without elastic tunneling (Lucas-Ewing mechanism[9]), i.e., putting $Q^{vv'}_{ci'}=0$, reduces the rates by about a factor of 3 at $T=100$ K and a factor of 10 at $T=50$ K (dotted curves in Fig. 4). Because this model potential has a wider range as compared to that for Fig. 3, the derivative pho-

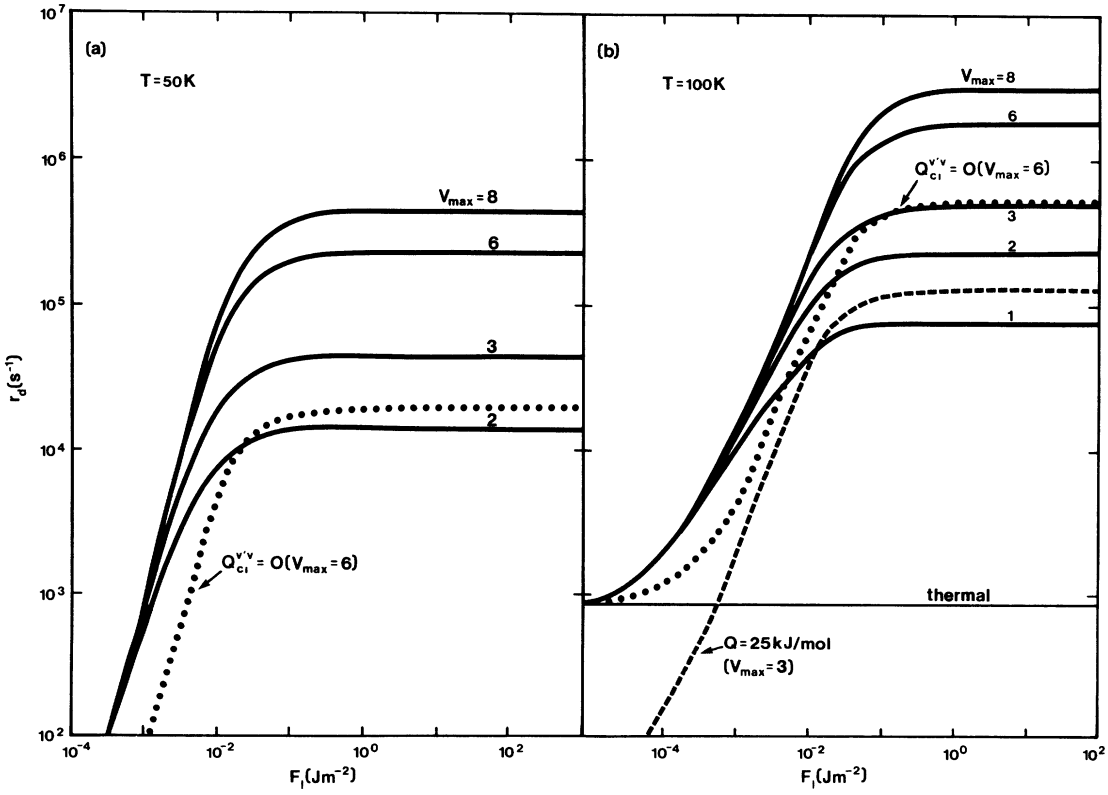

FIG. 4. As Fig. 3 but for $\sigma_0=22.82$, $r=53.7$. Dashed curve for $T=100$ K is for a deeper surface potential as indicated.

non coupling is weaker, making (temperature-independent) elastic tunneling more effective; higher temperature enhances inelastic tunneling, however.

In a fourth model for CH_3F-NaCl we kept the larger range of $\gamma^{-1}=0.35$ A and made the potential deeper again to correspond to a heat of adsorption of 25 kJ/mol. This now, not surprisingly, reduces the rates by about a factor of 4 as compared to the shallower potential.

We will now attempt a comparison of our model calculations with the experiment by Heidberg *et al.*[11,13] Looking at their Fig. 10 in Ref. 11 or Fig. 2 in Ref. 13 one is tempted to see an analogy with the left halves of our Figs. 3 and 4. In the experiment the remaining coverage $\theta=\theta(\tau_l)$ is determined after a laser flash of duration τ_l has desorbed a fraction $(\theta_0-\theta)$ with θ_0 being the initial coverage. Assuming an exponential decay $\theta=\theta_0\exp(-r_d t)$ one can extract from Fig. 2 in Ref. 12, desorption rates as a function of fluence as

$$r_d=\tau_l^{-1}\ln(\theta_0/\theta)$$

with τ_l given as 200 ns. At $F_l=800$ J m^{-2} their data yield $r_d\approx 5\times 10^5$ s^{-1}. Our theory (both models of Figs. 3 and 4) produces such values at much smaller fluences in the range $10^{-2}-10^{-1}$ J m^{-2}. There are several uncertainties that made a direct comparison difficult (and thus save our theory from outright rejection). (1) Our theory is made for the zero-coverage limit; at finite coverage (unknown in the experiment) dipole-dipole (v-v) coupling between adsorbed molecules will dissipate the absorbed laser energy slowing down desorption; experiment then needs a higher fluence at finite coverage than the theory needs at zero coverage to achieve the same desorption rate. (2) Our theory predicts that a lot of the laser energy is used up to resonantly heat the solid via inelastic bound-state—bound-state tunneling and subsequent phonon cascade in the surface potential. We have not yet calculated the resulting temperature rise which can lead to enhanced thermal desorption; we suggest that in the experiment the sample temperature is also measured after the laser pulses. (3) We have assumed in the theory that the CH_3F molecule sticks perpendicularly out from the surface. This is not known experimentally. Figure 2 suggests that, e.g., for an orientation of 60° with respect to the normal a laser intensity higher by about a factor of 2 is needed to give the same rate. (4) Last and most importantly we assumed that the dipole moment of CH_3F adsorbed onto NaCl is the same as that of the free molecule stemming from charges $\pm e$ at either end of the molecule. It is very likely that the dipole moment changes upon adsorption and a reduction of the effective charges to, e.g., $\pm 0.1e$ is quite possible. This would immediately raise our fluence values by a factor of 100 bringing them into line with the experiment. Though this is hopeful thinking, it is nevertheless quite possible, and we suggest that the dipole moment of adsorbed CH_3F be measured. For future comparisons between experiment and theory it would be very helpful if thermal desorption time also (without laser irradiation) could be measured, e.g., in temperature-programmed desorption experiments at two heating rates to allow a unique determination of heat of adsorption Q and prefactor ν in (57). This would allow the theorist to pin down with some confidence the depth and range parameters of the surface potential. Photodesorption experiments should also be done at a low and known coverage, e.g., at $\theta\lesssim 0.1$.

Our theory also allows us to estimate the linewidth Γ of the ν_3 molecular vibration of the adsorbed CH_3F molecule as it is given to a large extent by the inelastic tunneling transition probabilities $P_{i'i}^{01}$. For the model of Fig. 3 we find $\Gamma\approx 10^{11}$ s^{-1} ≈ 3 cm^{-1} and for the model of Fig. 4 we get $\Gamma\approx 10^9$ s$^{-1}\approx 0.03$ cm^{-1}. Experiments on other adsorbed molecules suggest[17] that typical linewidths are of order 5—50 cm^{-1} as compared to 0.001—0.1 in free molecules. A detailed account will be given elsewhere.[25]

B. CO on NaCl

Carbon monoxide adsorbs on NaCl with a heat of adsorption[26] of $Q=18$ kJ/mol=2170 K/particle. The C-O stretch vibration is increased[26] from 2143 cm^{-1} in free space to 2160 cm^{-1} in the adsorbed states at a coverage $\theta=0.1$. This implies that a single laser photon of that frequency can lift a CO molecule into a state degenerate with a continuum of CO in its vibrational ground state. We have modeled the CO-NaCl system by choosing a range of the surface potential $\gamma^{-1}=0.32$ Å so that $\sigma_0=16.13$ and $r=33.6$ implying that the lowest-two bound states are separated by $E_1-E_0\approx 0.9\hbar\omega_D$. Thermal desorption rates, calculated from (51) with the laser switched off, yield a prefactor $\nu=10^{14}$ s^{-1}. In Fig. 5 we plot the photodesorption rates r_d versus inverse temperature T^{-1} for various cutoffs $v_{\max}$ of the harmonic oscillator modeling the CO stretch vibration. One gets saturation for all fluences F_l less than 10^{-3} J m^{-2}, assuming again effective charges $\pm e$ on C and O ends of the adsorbed CO molecules. For temperatures $T\gtrsim 100$ K desorption is purely thermal; it becomes laser dominated very quickly for $T<100$ K. The very low fluences needed for saturation imply that laser-induced resonant desorp-

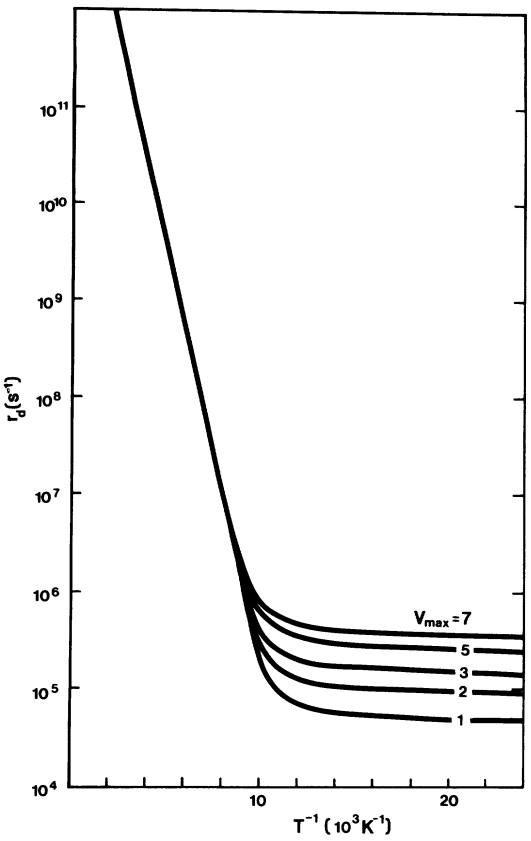

FIG. 5. Photodesorption rate for CO on NaCl. $\sigma_0=17$, $r=33$ vs inverse temperature for fluences $F_l > 10^{-2}\,\mathrm{J\,m^{-2}}$ (saturation).

tion of CO from NaCl could be attempted with a (1—10)-W laser operating in continuous mode.

VI. COMMENTS

In this paper we have developed a quantum-statistical theory of resonant photodesorption of molecules from the surface of dielectrics. The approach is based on the master equation (51) with the transition probabilities calculated according to Fermi's golden rule from the Hamiltonian (32). The numerical study, apart from providing photodesorption rates, highlighted three points: (1) the importance of resonant heating through inelastic tunneling between bound states; (2) the importance of elastic tunneling[9] into the continuum for desorption; and (3) saturation of the photodesorption rates for high laser intensities as a function of the maximal number $v_{\max}$ of vibrational molecular states included. A number of experiments are suggested by this study: (1) thermal desorption experiments (e.g., temperature programmed) should be performed on the CH_3F-NaCl and CO-NaCl systems to allow a (rough) determination of the range of the surface potential from the prefactor ν given in (57) with the heat of adsorption Q measured calorimetrically. (2) The anharmonicity and linewidths of the ν_3 vibration of the adsorbed CH_3F molecule and its dipole moment should be measured to pin down some of the parameters entering a theory of resonant photodesorption. (3) Lower laser intensities are needed to reach saturation in the CO-NaCl system according to Fig. 5, and experiment should therefore be easier. (4) The higher vibrational excitations in the saturation regime might be detected as additional maxima in the time of flight spectrum at times of arrival

$$t_v \sim l/[2m(v+\tfrac{1}{2})\hbar\Omega - Q]^{1/2}$$

for v large enough, where l is the flight path to the detector. The spectrum, of course will differ strongly from a quasi-Maxwellian spectrum usually observed in thermal desorption.

In the theory a number of further calculations will be performed: (1) We will calculate explicitly the resonant heating rate. (2) We will make a detailed study of the linewidths of the vibrational levels of the adsorbed molecule. Improvements of the theory must include: (1) a three-dimensional version of the so far one-dimensional theory; this is possible with the experiences gained in previous work, e.g., in Ref. 20. (2) With the methods developed in Ref. 24 one should include two-phonon processes in the calculation of transition probabilities. (3) One would hope that the full master equation (51) can be simplified into a simpler approximate equation in the same way as we reduced the master equation of the thermal-desorption cascade model to Fokker-Planck and Kramers equations in Refs. 27 and 28. This would make the theory more pallable to experimentalists. (4) So far our theory was restricted to adsorbates of vanishing coverage. An extension to finite coverage must take the dipole-dipole interaction between coadsorbed molecules into account. One hopes that now after priorities have been established more careful experiments will also present data on the coverage at which photodesorption is measured. (5) After a careful study of electromagnetic fields at metal surface an extension of the present theory, so far restricted to dielectrics, will be given.

ACKNOWLEDGMENTS

This work was supported in part by a grant from the Natural Sciences and Engineering Council of Canada. One of us (H.J.K.) would like to thank Profesor G. Wedler for many stimulating discussions during his (H.J.K.) stay in Erlangen during the summer semester, 1982. Thanks are also due to Professor J. Heidberg and Dr. I. Hussla for discussions and for providing unpublished data.

APPENDIX

In this appendix we summarize the essential features of the electromagnetic fields at the surface of a dielectric including their quantization. We consider light incident from the vacuum side under an angle θ_i with respect to the surface normal $\vec{n}$. The normal modes of radiation are calculated from Maxwell's equations with appropriate boundary conditions. Their wave vector $\vec{k}=(\vec{K},\kappa)$ is decomposed into a two-dimensional component $\vec{K}$ parallel to the surface and its z component $\kappa<0$ perpendicular to it. Their polarization Π can be decomposed into two independent ones: $\Pi=s$ polarized perpendicular to the plane of incidence (s waves or TE waves) and $\Pi=p$ polarized in this plane (p waves of TM waves). The vector potential is then given by

$$\vec{A}(\vec{R},z)=\sum_{\vec{K},\Pi}\int_{-\infty}^{0}d\kappa[\hbar/2\epsilon_0\Omega(\vec{K},\kappa)]^{1/2}[\vec{U}^{(\Pi)}_{\vec{K},\kappa}(\vec{R},z)e^{-i\Omega(\vec{K},\kappa)t}c^{(\Pi)}_{\vec{K},\kappa}+\text{c.c.}]\ , \tag{A1}$$

where c.c. denotes complex conjugate. We also have

$$\vec{U}^{(s)}_{\vec{K},\kappa}(\vec{R},z)=(2\pi S)^{-1/2}e^{i\vec{K}\cdot\vec{R}}(\vec{n}\times\vec{K}/K)\{\Theta(z)[e^{i\kappa z}+e^{-i\kappa z}(1-n_r a)/(1+n_r a)]+\Theta(-z)2e^{-i\kappa z}/(1+n_r a)\}\ , \tag{A2}$$

$$\begin{aligned}\vec{U}^{(p)}_{\vec{K},\kappa}(\vec{R},z)=&(2\pi S)^{-1/2}e^{i\vec{K}\cdot\vec{R}}(n_r+a)(K^2+\kappa^2)^{-1/2}\\&\times(n_r^2+2an_r+a^2)^{-1/2}\left[\Theta(z)\left[\vec{n}K\left[e^{i\kappa z}+e^{-i\kappa z}\frac{n_r-a}{n_r+a}\right]\right.\right.\\&\left.\left.-\frac{\vec{K}}{K}\kappa\left[e^{i\kappa z}-e^{-i\kappa z}\frac{n_r+a}{n_r-a}\right]+\Theta(-z)\left[2e^{-i\kappa z}\frac{K\vec{n}-n_r\kappa a\vec{K}/K}{n_r+a}\right]\right]\right],\end{aligned} \tag{A3}$$

where S is the surface area, $a=\cos\theta_t/\cos\theta_i$, with θ_t the angle between the transmitted beam and the negative surface normal. Also $\Theta(z)=1$ for $z\geq 0$ and $\Theta(z)=0$ for $z<0$. n_r is the refractive index of the dielectric. These modes satisfy the orthogonality relations

$$\int d\vec{R}\int_{-\infty}^{\infty}dz[n_r\Theta(-z)+\Theta(z)]^2\vec{U}^{(\Pi')*}_{\vec{K}',\kappa'}(\vec{R},z)\vec{U}^{(\Pi)}_{\vec{K},\kappa}(\vec{R},z)=\delta_{\Pi'\Pi}\delta_{\vec{K}',\vec{K}}\delta(\kappa'-\kappa)\ . \tag{A4}$$

To quantize the electromagnetic field we simply treat the expansion coefficients $c^{(\Pi)}_{\vec{K},\kappa}$ as annihilation operators satisfying Bose-Einstein commutation relations. In the evaluation of the laser transition probabilities (35) one needs the normal modes (A3) taken at $\vec{R}=0$ and $z=0^+$. In (39) only its incident part proportional to $\exp(i\kappa z)$ is used. In Sec. IV A we considered a situation where the dipole moment $\vec{\mu}$ of the adsorbed molecule is perpendicular to the surface. If it forms an angle θ_m with the normal and ϕ_m with respect to some direction in the surface plane then the coupling of the laser, incident under an angle θ_i, into the dipole, averaged over ϕ_m on a uniform surface, is proportional to

$$\begin{aligned}\langle|\vec{E}\cdot\vec{\mu}|^2\rangle/|\vec{E}^{(p)}|^2=&2(I^{(s)}_{\text{inc}}/I^{(p)}_{\text{inc}})\sin^2\theta_m\cos^2\theta_i[(n_r^2-\sin^2\theta_i)^{1/2}+\cos\theta_i]^{-2}\\&+2\cos^2\theta_i[(n_r^2-\sin^2\theta_i)^{1/2}+n_r^2\cos\theta_i]^{-2}[(n_r^2-\sin^2\theta_i)\sin^2\theta_m+2n_r^4\sin^2\theta_i\cos^2\theta_m]\ .\end{aligned} \tag{A5}$$

For $\theta_m=0$ this reduces to the angular dependence of (43).

[1]L. P. Levine, J. F. Ready, and E. Bernal G., J. Appl. Phys. 38, 331 (1967).
[2]L. P. Levine, J. F. Ready and E. Bernal G., IEEE J. Quantum Electron. QE4, 18 (1968).
[3]G. Ertl and M. Neumann, Z. Naturforsch. Teil A 27, 1607 (1972).
[4]M. Neumann Ph.D. thesis, University of Hannover, 1973 (unpublished).
[5]K. Christmann, D. Schober, G. Ertly, and M. Neumann, J. Chem. Phys. 60, 4528 (1974).
[6]G. Wedler and H. Ruhmann, Surf. Sci. 121, 464 (1982).
[7]C. Jedrzejek, K. F. Freed, S. Efrima, and H. Metiu, Surf. Sci. 109, 191 (1981).
[8]This process has also been studied by J. Lin and T. F.

George, Chem. Phys. Lett. 66, 5 (1979); latest in a series is Surf. Sci. 115, 569 (1982).
[9]D. Lucas and G. E. Ewing, Chem. Phys. 58, 385 (1981).
[10]H. J. Kreuzer and D. N. Lowy, Chem. Phys. Lett. 78, 50 (1981).
[11]J. Heidberg, H. Stein, A. Nestmann, E. Hoefs, and I. Hussla, in *Laser-Solid Interactions and Laser Processing—1978 (Materials Research Society, Boston)*, Proceedings of the Symposium on Laser-Solid Interactions and Laser Processing, edited by S. D. Ferris, H. J. Leamy, and J. M. Poate (AIP, New York, 1979), p. 49.
[12]J. Heidberg, H. Stein, E. Riehl, and A. Nestmann, Z. Phys. Chem. Neue Folge 121, 145 (1980).
[13]J. Heidberg, H. Stein, and E. Riehl, Phys. Rev. Lett. 49, 666 (1982).
[14]T. J. Chuang, J. Chem. Phys. 76, 3828 (1982).
[15]T. J. Chuang and H. Seki, Phys. Rev. Lett. 49, 382 (1982).
[16]R. G. Greenler, J. Chem. Phys. 44, 310 (1966).
[17]For a recent review of infrared absorption and reflection spectroscopy see A. M. Bradshaw, Appl. Surf. Sci. 11/12, 712 (1982).
[18]M. Fleishman, P. J. Hendra, and A. J. McQuillan, Chem. Phys. Lett. 26, 163 (1974).
[19]For a recent contribution, see D. L. Mills and M. Weber, Phys. Rev. B 26, 1075 (1982).
[20]Thermal desorption mediated by proper surface modes has been calculated by E. Goldys, Z. W. Gortel, and H. J. Kreuzer, Solid State Commun. 40, 963 (1981); Surf. Sci. 116, 33 (1982); also see J. Stutzki and W. Brenig, Z. Phys. B 45, 49 (1981).
[21]Z. W. Gortel, H. J. Kreuzer, and R. Teshima, Phys. Rev. B 22, 5655 (1980).
[22]I. Hussla (private communication).
[23]G. M. Barrow, Proc. R. Soc. London Ser. A 213, 27 (1952).
[24]Z. W. Gortel, H. J. Kreuzer, and R. Teshima, Phys. Rev. B 22, 512 (1980).
[25]Electronic damping of adsorbate vibrations on metal surfaces has been calculated by M. Perrson and B. Hellsing, Phys. Rev. Lett. 49, 662 (1982).
[26]I. Hussla, Ph.D. thesis, University of Erlangen-Nürnberg, 1980 (unpublished).
[27]Z. W. Gortel, H. J. Kreuzer, R. Teshima, and L. A. Turski, Phys. Rev. B 24, 4456 (1981).
[28]H. J. Kreuzer and R. Teshima, Phys. Rev. B 24, 4470 (1981).